

Ray Valencia  
Timm Denecke  
Lukas Lehmkuhl  
Frank Fischbach  
Roland Felix  
Friedrich Knollmann

## Value of axial and coronal maximum intensity projection (MIP) images in the detection of pulmonary nodules by multislice spiral CT: comparison with axial 1-mm and 5-mm slices

Received: 30 March 2005  
Revised: 11 June 2005  
Accepted: 8 July 2005  
Published online: 16 August 2005  
© Springer-Verlag 2005

R. Valencia (✉) · T. Denecke ·  
L. Lehmkuhl · F. Fischbach · R. Felix ·  
F. Knollmann  
Klinik für Strahlenheilkunde,  
Campus Virchow-Klinikum,  
Charité-Universitätsmedizin Berlin,  
Berlin, Germany  
e-mail: vray@gmx.net  
Tel.: +49-30-450557002  
Fax: +49-30-450557901

**Abstract** The purpose of this study was to investigate the diagnostic accuracy of non-overlapping 10-mm axial and coronal maximum intensity projections (MIP) in comparison with standard axial 1-mm and 5-mm slices in the detection of pulmonary nodules. Sixty patients with suspected nodules who underwent multislice spiral CT of the chest were evaluated. Axial 1-mm and 5-mm slices as well as non-overlapping 10-mm axial/coronal MIPs were interpreted independently by three blinded radiologists. After initial review, a retrospective consensus session was performed for agreement on final nodule counts using the axial 1-mm slices as gold standard. Small nodules of less than 5 mm in size were most accurately detected by the axial MIPs. Receiver operating

characteristic (ROC) analysis of these small nodules showed that 5-mm slices were not capable of a statistically significant differentiation of nodules from other focal lesions in two observers ( $p=0.034$  and  $p=0.012$ , respectively) whereas 1-mm slices and coronal/axial MIPs did allow a statistically significant differentiation in all observers ( $p<0.001$ ). Nodules larger than 5 mm were equally well depicted with all modalities. Non-overlapping 10-mm axial MIPs improve the accuracy in the detection of small pulmonary nodules.

**Keywords** Maximum intensity projection · MIP · Pulmonary nodule · Thoracic CT · Multislice computed tomography

### Introduction

The pulmonary nodule is one of the most common findings at computed tomography (CT) examinations. In 1996, the Fleischner Society published a glossary of terms specifically for thoracic CT in which a pulmonary nodule was defined as a round opacity, at least moderately well marginated and no greater than 3 cm in maximum diameter [1].

Particularly since the introduction of spiral technology, CT is the preferred modality for imaging pulmonary nodules [2, 3]. Spiral CT technology enabled a further increase in Z-axis coverage and acquisition of thin-slice images of the whole lung with a slice thickness in the range of 1 mm. Thin collimation increases spatial resolution, reduces partial-volume effects and allows an improved

detection of small pulmonary nodules [4]. However, high diagnostic expenditure and low diagnostic confidence in the detection of small pulmonary nodules (largest diameter  $\leq 10$  mm) by multislice spiral CT are still widespread and common problems. The overall sensitivity for nodule depiction is determined by technical parameters as well as the variability among observers to actually detect nodules depicted on the images [5]. Although lesions may be missed if slice thickness exceeds nodule diameter and a reduction of slice thickness should therefore improve sensitivity for pulmonary nodule detection, there are still several factors limiting an adequate diagnostic work-up. First, the reduction of slice thickness results in a prohibitive number of images, especially when combined with an overlapping image reconstruction [5–7]. The large number

of images to be interpreted may have a negative effect on observer vigilance and may therefore cause false-negative findings. Second, the problem of an accurate differentiation between pulmonary vessels or scars depicted in cross-section and small pulmonary nodules is aggravated [5, 6].

To date, several studies have demonstrated the incremental benefit of maximum intensity projections (MIP), especially in the depiction of small pulmonary nodules, using an overlapping MIP technique with varying reconstruction intervals [5–8]. Most of these studies have evaluated images with a collimation of more than 3 mm [5–7] or were limited to the evaluation of a small portion of the lung [9]. Only one study has been published so far performing a comparison between the diagnostic accuracy of axial image review with a slice thickness of 5 mm as compared with MIP image review with a slab thickness of 5 mm displayed in axial and coronal reformations, followed by a retrospective correlation with 1-mm slice review [8].

To the best of our knowledge, no study has been published so far evaluating non-overlapping axial and coronal 10-mm MIP images generated from axial 1-mm-thin collimation slices. Hence, the purpose of this study was to investigate the feasibility and diagnostic accuracy of coronal and axial 10-mm non-overlapping MIPs in direct comparison with axial 1-mm and 5-mm slices in the detection of pulmonary nodules.

## Materials and methods

### Patients

This study encompassed clinically indicated routine chest CT studies of 60 consecutive patients (28 men, 32 women; age range, 10–81 years; mean age, 49 years) who were referred for CT assessment for various reasons (primary lung tumor,  $n=3$ ; extrathoracic malignancy,  $n=39$ ; nonspecific inflammation,  $n=18$ ) with a likelihood to display small pulmonary nodules. The study was conducted according to the declaration of Helsinki.

### Image acquisition and reconstruction

The examinations were performed on a multislice CT scanner (Somatom Plus 4 VolumeZoom, Siemens, Erlangen, Germany) according to our standard protocol for chest examinations. After informed consent was obtained, intravenous contrast agent (100 ml Ultravist-370/Schering, Berlin, Germany) was administered using an injection rate of 2.5 ml/s. Scan acquisition parameters were identical in all patients (scan delay, 40 s; single breath hold; 140 kV; 120 mAs (effective mAs); collimation, 1 mm). Thin-slice sections were reconstructed with a high-resolution reconstruction algorithm. Axial scans were reconstructed from

the raw data with 1-mm and 5-mm slice thickness (slice thickness = reconstruction increment). Axial and coronal MIPs were reconstructed from the initial axial images on a workstation (Advantage Windows 4.1, General Electric Health Care, Milwaukee, WI, USA) with a slab thickness of 10-mm and 10-mm reconstruction increment. All images were displayed with window and center settings appropriate for lung parenchyma evaluation (level –600 HU, width level 1,600 HU).

### Image analysis

Initial image interpretation was performed independently by three blinded radiologists experienced in thoracic CT (RV, TD, LL). The observers recorded the number, size and exact location of every pulmonary nodule as well as the level of diagnostic confidence according to a 5-point confidence level scale (1, no nodule; 2, no confident nodule; 3, probable nodule; 4, more definite nodule; 5, definite nodule) on a standardized form. A pulmonary nodule was defined as a round opacity at least moderately well marginated and no greater than 3 cm in maximum diameter [1]. Pleural nodules or lesions with a differential diagnosis of scarring or misinterpretation of pulmonary vessels were classified with a confidence level of 1, as were ground-glass opacities. The nodules were categorized into three size classes (1, <5 mm; 2, 5–10 mm; 3, >10 mm). For size measurement, the largest diameter in the transverse plane was assessed. All image review was performed on a workstation (Advantage Windows, General Electric Health Care) in cine mode. To avoid a negative effect on the reviewer's vigilance, not more than five patients were investigated per day, especially for 1-mm readings. There were no restrictions on reading time. A minimum interval of 1 week between analyses of the different modalities (1-mm, 5-mm slices, axial, coronal MIPs) from the same patient by the same reader was defined in order to avoid recognition of pathologies. Scans were offered to the observers in a randomized order. After the initial independent review, a consensus session for retrospective nodule review, correlation, and classification was performed by all observers for agreement on final nodule counts using the axial 1-mm slices as gold standard. Patients with more than six nodules were classified as having diffuse disease and were excluded from the study since a thorough evaluation of the exact number and location of nodules seems impracticable in these instances.

### Statistical analysis

Statistical analysis was performed by using the statistical software program SPSS for Windows (Version 10.0.7/SPSS Inc., Chicago, IL, USA). As an index for concordance concerning the nodules detected and the assignment

**Table 1** Number of nodules with a confidence level of 2–5 detected by the observers using the different image review modalities as compared with the “true” consensus values. *MIP* maximum intensity projection

Nodule size	No. of nodules/modality			
	1 mm	5 mm	Coronal MIP	Axial MIP
<b>Observer 1</b>				
<5 mm	42	47	52	63
5–10 mm	13	13	11	14
>10 mm	14	13	11	14
Total	69	73	74	91
<b>Observer 2</b>				
<5 mm	39	46	61	73
5–10 mm	15	15	15	15
>10 mm	14	14	14	15
Total	68	75	90	103
<b>Observer 3</b>				
<5 mm	37	43	64	61
5–10 mm	13	14	9	15
>10 mm	14	15	13	14
Total	64	72	86	90
<b>True consensus values</b>				
<5 mm			68	
5–10 mm			14	
>10 mm			14	
Total			96	

of confidence scores, Pearson’s test ( $r$ , correlation coefficient) was used. For evaluation of observer performance in distinguishing pulmonary nodules from scars and vessels according to the confidence scores, receiver operating characteristic (ROC) analysis was used for each observer when using the different modalities (1-mm slices, 5-mm slices, axial MIP, coronal MIP). The area under the curve (AUC) was used to compare the performance of the different display modalities in the detection and accurate differentiation of pulmonary nodules from other focal pulmonary lesions. The confidence interval was set at 99.5%, and  $p$  values of  $\leq 0.005$  were accepted as statistically significant. Analyses were performed for all pulmonary nodules together and again separately for nodules of every size class.

**Table 2** Interobserver agreement for nodule detection and classification as calculated by the Pearson test, subdivided into nodule size classes and review modalities

Nodule size	Mean $r$ values (range)/modality			
	1 mm	5 mm	Coronal MIP	Axial MIP
<5 mm	0.695 (0.636–0.759)	0.694 (0.619–0.735)	0.687 (0.672–0.703)	0.751 (0.680–0.790)
5–10 mm	0.632 (0.560–0.712)	0.541 (0.499–0.610)	0.599 (0.514–0.733)	0.884 (0.861–0.920)
>10 mm	0.924 (0.886–1.0)	0.846 (0.777–0.886)	0.924 (0.886–1.0)	0.918 (0.877–1.0)

*MIP* maximum intensity projections

## Results

### Number of detected nodules

The observers correspondingly identified five patients as having more than six pulmonary nodules; these patients were excluded from the study. In 20 patients, no nodules were found correspondingly by all observers in all image review modalities (1-mm slices, 5-mm slices, coronal MIP, axial MIP). In 35 patients, the observers identified a total of 151 pulmonary nodules [size class 1, 104 nodules (69%); size class 2, 28 nodules (19%); size class 3, 19 nodules (12%)]. Table 1 shows the number of detected nodules per observer, nodule size and review modality. Of the 151 nodules detected by the three reviewers at initial image interpretation, 96 (64%) were classified as “true” pulmonary nodules (Table 1) and 55 (36%) as either pulmonary scars or pulmonary vessels (false positives) at the retrospective consensus reading. Thirty-six (65%) of the lesions classified as pulmonary scars or vessels were smaller than 5 mm in maximum diameter, 14 (25%) were in the size range of 5–10 mm and 5 (9%) measured more than 10 mm.

The mean number of images reviewed was 286 (range, 266–302) for the 1-mm slices, 61 (range, 53–64) for the 5-mm slices, 22 (range, 19–25) for the coronal MIPs and 28 (range, 26–31) for the axial MIPs.

### Interobserver agreement

Interobserver agreement for the detection and characterization of nodules of all size classes showed a mean  $r$  value of 0.722 (range, 0.683–0.745) for 1-mm slice review, 0.703 (range, 0.641–0.764) for 5-mm slice review, 0.743 (range, 0.716–0.789) for coronal MIP review, and 0.799 (range, 0.751–0.831) for axial MIP review, all indicating a good agreement. The  $r$  values for interobserver agreement subdivided into the different size classes and review modalities are shown in Table 2. Interobserver agreement was good in almost all modalities and size classes, except for nodules with a size of 5–10 mm, reviewed by 1-mm and 5-mm slices as well as coronal MIPs; here, interobserver agreement was only moderate (Table 2).

## Retrospective verification of nodules

The ROC curves for pulmonary nodules of all sizes as classified by the three observers on the different image presentation modalities are displayed in Fig. 1. The mean AUC for the three observers representing the feasibility of nodule differentiation was 0.769 (range, 0.741–0.824) for 1-mm slice review, 0.712 (range, 0.678–0.736) for 5-mm slice review, 0.867 (range, 0.836–0.892) for coronal MIPs, and 0.964 (range, 0.973–0.959) for axial MIPs. All review modalities allowed a statistically significant differentiation between pulmonary nodules and other lesions such as pulmonary scars or vessels ( $p < 0.001$ ). When stratifying the data for nodule size, the separate analysis of lesions  $> 10$  mm or 5–10 mm in diameter yielded similar results as compared with analysis of all sizes together; coronal and axial MIPs yielded higher AUC values as compared with 1-mm and 5-mm slices, and all modalities allowed a statistically significant differentiation between pulmonary nodules and other lesions such as pulmonary scars or vessels.

In contrast to the analysis of all nodule sizes together, the analysis of lesions smaller than 5 mm yielded the result that only 1-mm slices, coronal MIP, and axial MIP allowed a statistically significant differentiation of pulmonary nod-

ules ( $p \leq 0.001$ ). The  $p$  values for 5-mm slice review were not statistically significant in two observers ( $p = 0.034$  and  $p = 0.012$ , respectively), the  $p$  value found in the analysis of observer three was 0.004. Figure 2 shows the ROC curves for lesions with a maximum diameter of  $< 5$  mm for the three observers. The mean AUC was 0.731 (range, 0.692–0.809) for 1-mm slice review, 0.649 (range, 0.626–0.673) for 5-mm slice review, 0.870 (range, 0.844–0.890) for coronal MIP, and 0.961 (range, 0.949–0.973) for axial MIP.

Figures 3 and 4 display two examples of the incremental benefit of MIP review for the detection of small pulmonary nodules.

## Discussion

To date, a number of methods and display modes such as cine-based viewing [10], multiplanar reformations [11], computer aided diagnosis (CAD) [12–15], and the MIP technique [5–8] have been used and evaluated in order to enhance the radiologists' performance in pulmonary nodule detection and approach the problem of prohibitive image numbers. The effectiveness of double reading to improve sensitivity [16] and the influence of reader experience [15] have also been subject to recent research. The present study

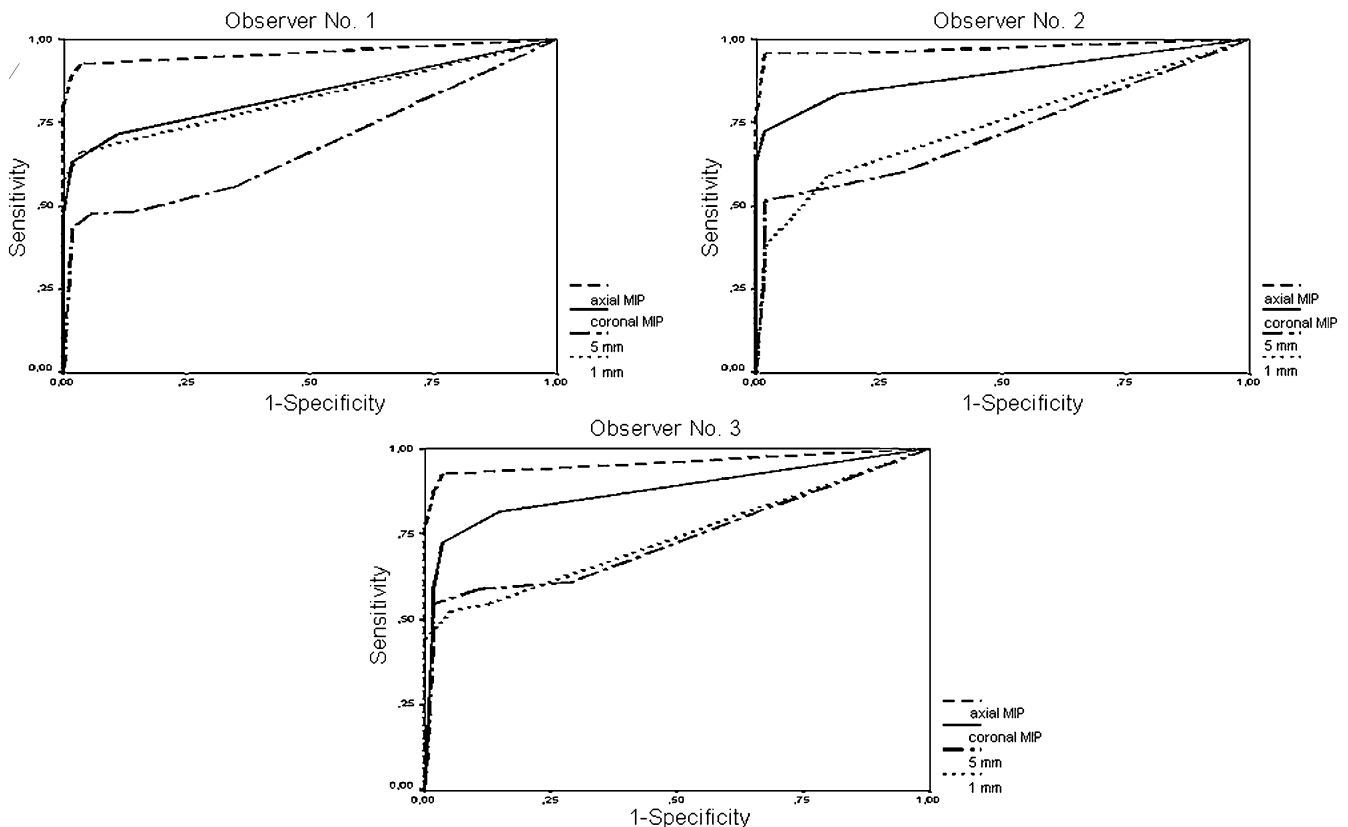


**Fig. 1** Receiver operating characteristic (ROC) curves for pulmonary nodules of all size classes subdivided into the different observers

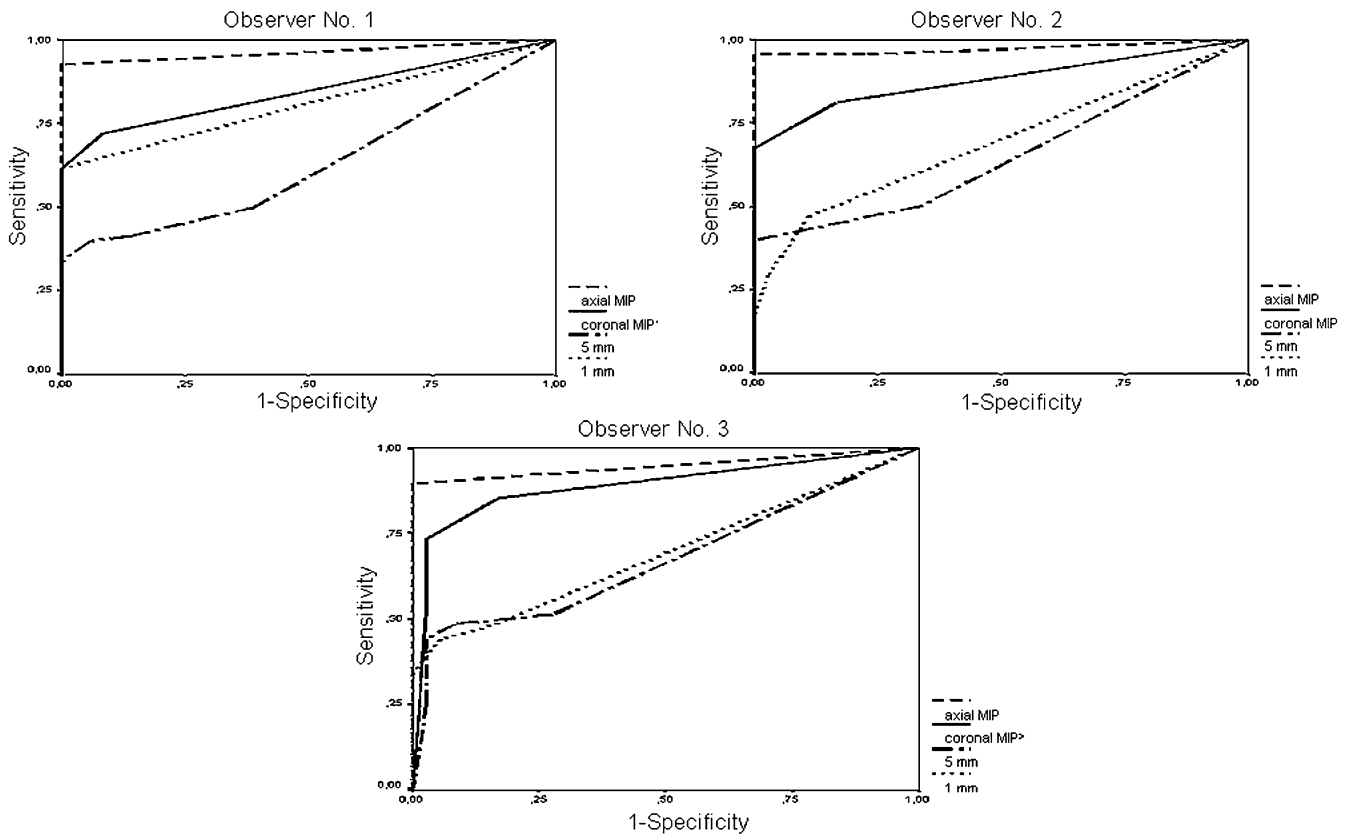


**Fig. 2** Receiver operating characteristic (ROC) curves for pulmonary nodules of less than 5 mm in size subdivided into the different observers

aimed at evaluating the diagnostic benefit of 10-mm coronal and axial MIPs in the detection of small pulmonary nodules as compared with standard 1-mm and 5-mm slice review, further lowering the number of images by using non-overlapping MIP slab reconstructions.

In our study, analysis of the nodule detection rates showed that the most striking differences between the review modalities were found in nodules smaller than 5 mm; nodules with a size of 5–10 mm and more than 10 mm were detected with similar frequencies by all review modalities. This finding is consistent with reports in the literature [4, 8]. All observers detected clearly more nodules with less than 5 mm in maximum diameter when reviewing the coronal and axial MIP images as compared with standard 1-mm and 5-mm slice review. ROC analysis of these small nodules showed that standard 5-mm slices were not capable of a statistically significant differentiation of pulmonary nodules from other focal lesions whereas 1-mm slice review, coronal, and axial MIP review did allow a statistically significant differentiation by all observers. This finding explains why more nodules of less than 5 mm in size were found in the initial 5-mm slice review as compared with 1-mm slice review; all additional nodules found in 5-mm

slice review were classified as pulmonary scars or vessels at the retrospective consensus session. Overall, the diagnostic accuracy in the detection of pulmonary nodules was lowest with 5-mm slice review.

To the best of our knowledge, no previously published study has performed a direct comparison between pulmonary nodule detection rates of standard axial 1-mm slices and MIP slabs. Eibel et al. have only conducted a comparison of standard axial 5-mm slices and multiplanar MIPs with a slab thickness of 5 mm, using the 1-mm slices as gold standard for retrospective nodule correlation and verification [8]. However, we have found that in direct comparison, axial and coronal MIPs proved to be superior to the 1-mm and 5-mm standard slices in the depiction and accurate diagnosis of small pulmonary nodules with a size of less than 5 mm, as indicated by higher nodule detection rates and a more accurate differentiation from other focal pulmonary lesions. This result is most likely due to the fact that observers tend to overlook small nodules depicted within a complex background [5] and due to the ability of MIP images to enable a clear differentiation of vascular and nodular structures. Furthermore, the interobserver agreement was best for axial MIP review. This finding is also

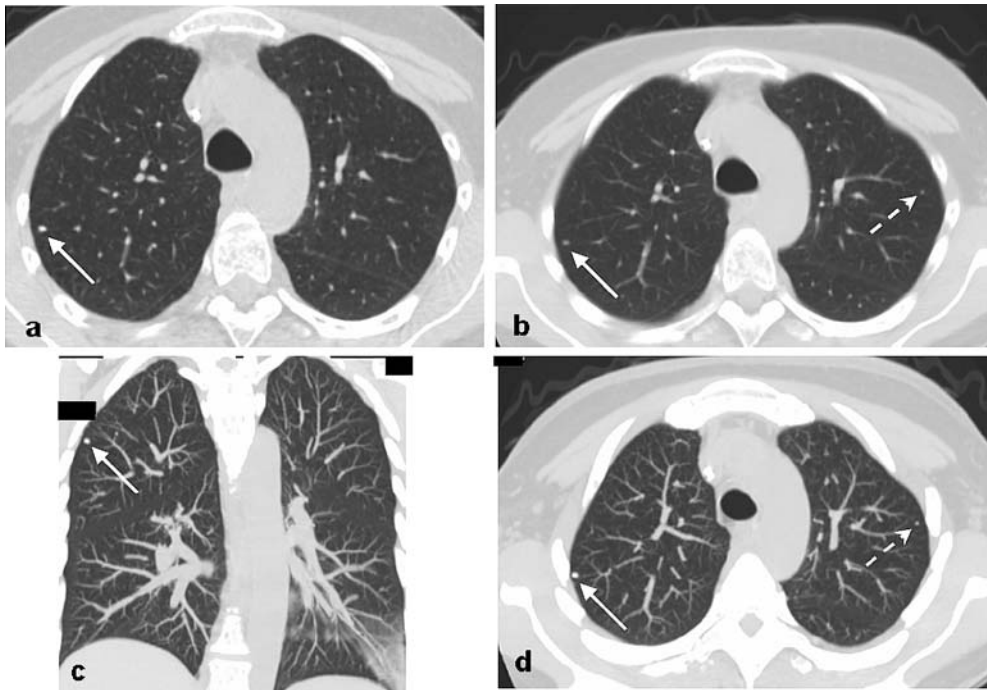


**Fig. 3** **a** Standard axial 1-mm slices show a small pulmonary nodule of 5 mm in diameter (*arrow*) in the right upper lobe confidently seen by all observers. **b** Standard axial 5-mm slices depict that same nodule in the right upper lobe, also confidently seen by all observers, and an additional small pulmonary nodule of 2 mm in diameter (*striped arrow*) in the left upper lobe initially overlooked by all observers. **c** Coronal 10-mm maximum intensity projection (MIP) images enabled a confident diagnosis of the nodule depicted

in the right upper lobe; the nodule in the left upper lobe was also confidently seen by all observers on another image number (image not depicted). **d** Axial 10-mm MIP images allowed a confident diagnosis of both nodules (*arrows*) by all observers on one single image. The nodule in the left upper lobe (*striped arrow*) was identified only retrospectively in the standard axial 1-mm (image not depicted) and 5-mm slices

emphasized by Gruden et al. who concluded that the MIP technique is able to eliminate some of the interobserver variability in the detection of pulmonary nodules [5].

Eighty-eight percent of the nodules detected in our study were smaller than 10 mm. This figure is closely within the range published in the literature since small pulmonary nodules  $\leq 10$  mm have been reported in 89–97% of nodules detected in lung cancer screening studies of asymptomatic populations at risk [17–19]. In addition, these studies using low-radiation-dose CT have found that a small pulmonary nodule is an extremely common finding, proving to be benign in more than 95% of cases [17, 18].

Although there is considerable agreement in the literature that a small pulmonary nodule must not automatically be considered to be potentially malignant and that nodules smaller than 5 mm may be of only limited clinical relevance [13, 20, 21], any nodule detected at an early stage may offer the opportunity for an improved treatment in patients with malignant disease [4, 22].

The widespread use of multislice CT with the possibility to acquire image data of the whole lung with images comprised of isotropic voxels with a spatial resolution of 1 mm and less has led to an increased detection rate of small

pulmonary nodules [4]. However, significant limitations exist in the assessment of these small nodules with CT, and sensitivities of under 70% for such lesions have been reported in the literature [23, 24]. The present study underlines the great value of MIPs, especially in the detection of small pulmonary nodules, as previously reported by other authors [5–8].

MIP images are generated from an axial slab of volumetric data and have two major advantages. First, MIP images allow a clear differentiation of vascular and nodular structures since the vascular contiguity is depicted in a single image. Second, it is possible to preserve the spatial resolution of the axial thin slices from which the MIP slabs are created while markedly reducing final image numbers. In our study, the average number of axial MIP images per patient was reduced by 90% in comparison to the standard axial 1-mm slices.

The advent of multislice CT scanners has greatly affected the practice of CT since these scanners generate an enormous amount of image data per examination [25] and increase patient throughput at the same time [26]. Particularly if multiple studies must be interpreted, even with cine-based review, a number of images as low as

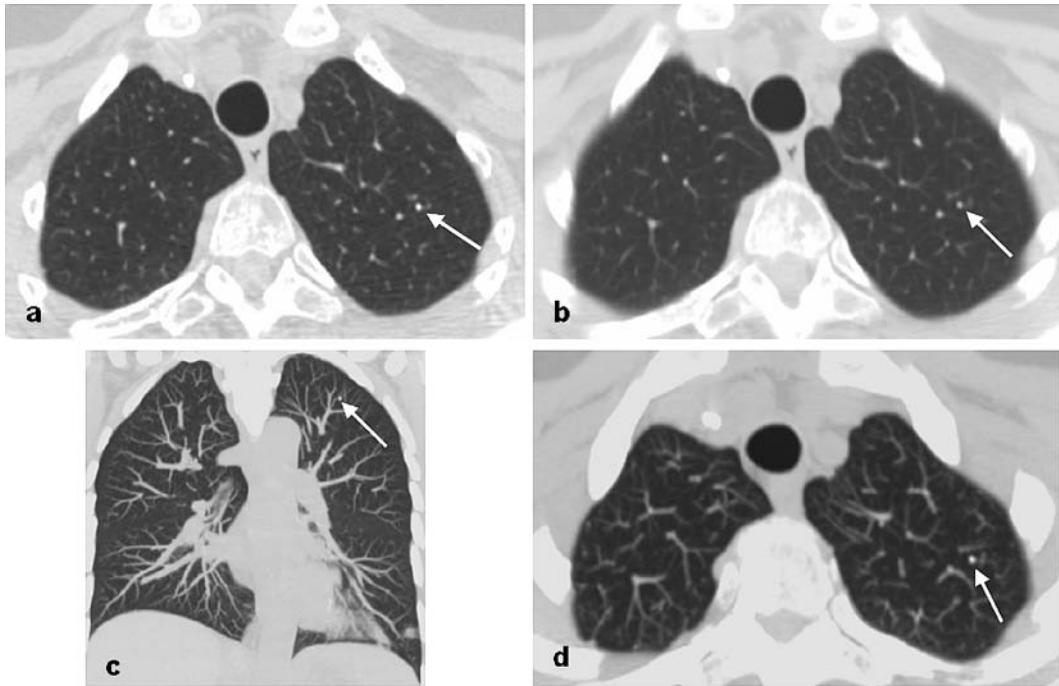


**Fig. 4** Small pulmonary nodule of 2 mm in diameter in the left upper lobe: **a, b** All observers overlooked the nodule (*arrow*) at initial standard axial 1-mm and 5-mm slice review; it was identified only retrospectively. **c** Coronal 10-mm maximum intensity projection (MIP) images enabled a confident diagnosis of the nodule

depicted in the left upper lobe (*arrow*) by all observers and allowed a precise differentiation from pulmonary vessels. **d** Axial 10-mm MIP images readily depicted the nodule (*arrow*) and allowed a confident diagnosis by all observers

reasonably achievable is desirable in order to enhance viewing conditions, preserving diagnostic accuracy [5–7]. In case of film-based image review, this issue is of even greater importance. In contrast to other studies evaluating the MIP technique in the detection of pulmonary nodules [5–8], we used non-overlapping slab reconstructions in order to further decrease the number of images and were able to demonstrate the feasibility of this method.

Another possibility to achieve a decrease in the number of images to be interpreted would be to increase the MIP slab thickness. However, thick MIPs of 30-mm slab thickness have been evaluated previously by other authors, and it has been shown that an increase of slab thickness decreases the accuracy in nodule detection due to a possible projection of nodules on pulmonary vessels [6]. Even with axial MIPs of 10-mm slab thickness, it is not unlikely that a 5-mm vessel running within the plane (e.g., upper lobe artery) might obscure a nodule of <5 mm located exactly above or below within the same slab. In coronal MIPs, the same applies for tiny nodules located in front of or behind a vertical vessel. Although this may not occur often in clinical situations and we did not experience this problem in our study, this principle limitation of the MIP technique should be mentioned. In our study, we aimed at finding a balance between low image numbers and a high diagnostic

accuracy and therefore chose an MIP slab thickness of 10 mm.

There are several limitations in our study design. First, as in many studies investigating the detection of pulmonary nodules with CT, there was no true gold standard for the detected nodules because surgical treatment and histological verification of the lesions were not performed. Instead, the results of the retrospective consensus session served as a reference standard, and there is no proof as to whether the observers accurately identified “true” pulmonary nodules. Histological verification and clinical follow-up of patients for assessment of nodule growth patterns would be mandatory to identify “true” nodules and false-negative findings [12]. Second, a direct comparison with the use of overlapping image reconstructions was not performed; therefore, possible differences in these techniques could not be evaluated.

In conclusion, our results indicate that axial MIP images are superior to axial 1-mm and 5-mm slices as well as coronal MIP images, yielding improved nodule detection rates and allowing a more accurate diagnosis of pulmonary nodules. On the basis of the findings presented in our study and on the basis of the results published in the literature concerning the MIP technique [5–9], the study protocol for evaluation of pulmonary nodules has been changed at our

institution. For assessment of pulmonary nodules, axial, non-overlapping, 10-mm MIP images are now primarily viewed, followed by a directed and focused review of standard 1-mm slices in case of suspicious or unclear lesions.

Intensive research especially on combinations of different image review methods (e.g., a combination of CAD and the MIP technique) is necessary to further approach the issue of imperfect nodule detection at chest CT examinations.

## References

- Austin JH, Muller NL, Friedman PJ, Hansell DM, Naidich DP, Remy-Jardin M, Webb WR, Zerhouni EA (1996) Glossary of terms for CT of the lungs: recommendations of the Nomenclature Committee of the Fleischner Society. *Radiology* 200:327–331
- Remy-Jardin M, Remy J, Giraud F, Marquette CH (1993) Pulmonary nodules: detection with thick-section spiral CT versus conventional CT. *Radiology* 187:513–520
- Tan BB, Flaherty KR, Kazerooni EA, Iannettoni MD (2003) The solitary pulmonary nodule. *Chest* 123:89S–96S
- Fischbach F, Knollmann F, Griesshaber V, Freund T, Akkol E, Felix R (2003) Detection of pulmonary nodules by multislice computed tomography: improved detection rate with reduced slice thickness. *Eur Radiol* 13:2378–2383
- Gruden JF, Ouanounou S, Tigges S, Norris SD, Klausner TS (2002) Incremental benefit of maximum-intensity-projection images on observer detection of small pulmonary nodules revealed by multidetector CT. *Am J Roentgenol* 179:149–157
- Diederich S, Lentschig MG, Overbeck TR, Wormanns D, Heindel W (2001) Detection of pulmonary nodules at spiral CT: comparison of maximum intensity projection sliding slabs and single-image reporting. *Eur Radiol* 11:1345–1350
- Coakley FV, Cohen MD, Johnson MS, Gonin R, Hanna MP (1998) Maximum intensity projection images in the detection of simulated pulmonary nodules by spiral CT. *Br J Radiol* 71:135–140
- Eibel R, Turk TR, Kulinna C, Herrmann K, Reiser MF (2001) Multi-detector-row CT of the lungs: multiplanar reconstructions and maximum intensity projections for the detection of pulmonary nodules. *Rofo Fortschr Geb Rontgenstrahlen Neuen Bildgeb Verfahr* 173:815–821
- Remy-Jardin M, Remy J, Artaud D, Deschildre F, Duhamel A (1996) Diffuse infiltrative lung disease: clinical value of sliding-thin-slab maximum intensity projection CT scans in the detection of mild micronodular patterns. *Radiology* 200:333–339
- Seltzer SE, Judy PF, Adams DF, Jacobson FL, Stark P, Kikinis R, Swensson RG, Hooton S, Head B, Feldman U (1995) Spiral CT of the chest: comparison of cine and film-based viewing. *Radiology* 197:73–78
- Eibel R, Turk T, Kulinna C, Schopf UJ, Bruning R, Reiser MF (2001) Value of multiplanar reformations (MPR) in multi-slice spiral CT of the lung. *Rofo Fortschr Geb Rontgenstrahlen Neuen Bildgeb Verfahr* 173:57–64
- Awai K, Murao K, Ozawa A, Komi M, Hayakawa H, Hori S, Nishimura Y (2004) Pulmonary nodules at chest CT: effect of computer-aided diagnosis on radiologists' detection performance. *Radiology* 230:347–352
- Armato SG III, McLennan G, McNitt-Gray MF, Meyer CR, Yankelevitz D, Aberle DR, Henschke CI, Hoffman EA, Kazerooni EA, MacMahon H, Reeves AP, Croft BY, Clarke LP (2004) Lung image database consortium: developing a resource for the medical imaging research community. *Radiology* 232:739–748
- Marten K, Grillhösl A, Seyfarth T, Obenauer S, Rummeny EJ, Engelke C (2005) Computer-assisted detection of pulmonary nodules: evaluation of diagnostic performance using an expert knowledge-based detection system with variable reconstruction slice thickness settings. *Eur Radiol* 15:203–212
- Marten K, Seyfarth T, Auer F, Wiener E, Grillhösl A, Obenauer S, Rummeny EJ, Engelke C (2004) Computer-assisted detection of pulmonary nodules: performance evaluation of an expert knowledge-based detection system in consensus reading with experienced and inexperienced chest radiologists. *Eur Radiol* 14:1930–1938
- Wormanns D, Ludwig K, Beyer F, Heindel W, Diederich S (2005) Detection of pulmonary nodules at multirow-detector CT: effectiveness of double reading to improve sensitivity at standard-dose and low-dose chest CT. *Eur Radiol* 15:14–22
- Diederich S, Wormanns D, Semik M, Thomas M, Lenzen H, Roos N, Heindel W (2002) Screening for early lung cancer with low-dose spiral CT: prevalence in 817 asymptomatic smokers. *Radiology* 222:773–781
- Swensen SJ, Jett JR, Sloan JA, Midhun DE, Hartman TE, Sykes AM, Aughenbaugh GL, Zink FE, Hillman SL, Noetzel GR, Marks RS, Clayton AC, Pairello PC (2002) Screening for lung cancer with low-dose spiral computed tomography. *Am J Respir Crit Care Med* 165:508–513
- Henschke CI, McCauley DI, Yankelevitz DF, Naidich DP, McGuinness G, Miettinen OS, Libby DM, Pasmantier MW, Koizumi J, Altorki NK, Smith JP (1999) Early lung cancer action project: overall design and findings from baseline screening. *Lancet* 354:99–105
- Wormanns D, Diederich S (2004) Characterization of small pulmonary nodules by CT. *Eur Radiol* 14:1380–1391
- Benjamin MS, Drucker EA, McLoud TC, Shepard JA (2003) Small pulmonary nodules: detection at chest CT and outcome. *Radiology* 226:489–493
- Greene RE (1992) Missed lung nodules: lost opportunities for cancer cure. *Radiology* 182:8–9
- Diederich S, Semik M, Lentschig MG, Winter F, Scheld HH, Roos N, Bongartz G (1999) Helical CT of pulmonary nodules in patients with extrathoracic malignancy: CT-surgical correlation. *Am J Roentgenol* 172:353–360
- Wormanns D, Diederich S, Lentschig MG, Winter F, Heindel W (2000) Spiral CT of pulmonary nodules: interobserver variation in assessment of lesion size. *Eur Radiol* 10:710–713
- Rubin GD (2000) Data explosion: the challenge of multidetector-row CT. *Eur J Radiol* 36:74–80
- Jhaveri KS, Saini S, Levine LA, Piazza DJ, Doncaster RJ, Halpern EF, Jordan PF, Thrall JH (2001) Effect of multislice CT technology on scanner productivity. *Am J Roentgenol* 177:769–772